# Precision targeting of rhabdomyosarcoma by combining primary CAR NK cells and radiotherapy

Lisa Marie Reindl [ID] ,[1,2] Lida Jalili,[1] Tobias Bexte [ID] ,[1,3,4,5] Sabine Harenkamp,[5] Sophia Thul,[1,2] Stephanie Hehlgans [ID] ,[2,6] Alina Wallenwein,[7] Florian Rothweiler,[8] Jindrich Cinatl,[8] Martin Michaelis,[8,9] Halvard Bonig [ID] ,[5,10] Elise Gradhand,[3,11] Meike Vogler [ID] ,[3,4,7] Franz Rödel [ID] ,[2,4,6] Winfried S Wels [ID] ,[2,4,12] Evelyn Ullrich [ID] [1,2,3,4]

For numbered affiliations see end of article.

**Correspondence to**
Professor Evelyn Ullrich;
Evelyn@Ullrichlab.de

## ABSTRACT

**Background:** Rhabdomyosarcoma (RMS) is the most common type of soft-tissue sarcoma in children, and it remains a challenging cancer with poor outcomes in high-risk and metastatic patients. This study reports the use of epidermal growth factor receptor (EGFR)-targeted chimeric antigen receptor (CAR) natural killer (NK) cells in combination with radiotherapy as a novel immunotherapeutic approach for RMS treatment.

**Methods:** Primary human NK cells from healthy donors were engineered using lentiviral transduction to express a cetuximab-based EGFR-specific CAR. The ability of the engineered NK cells to lyse RMS cells was then assessed in vitro in RMS monolayers and spheroids, as well as against chemotherapy-resistant and primary patient-derived RMS cells. Migratory properties of NK cells were observed in a subcutaneous RMS xenograft model using in vivo imaging, and the efficacy of EGFR-CAR NK cells in combination with localized fractionated radiotherapy was analyzed.

**Results:** Primary human EGFR-CAR NK cells demonstrated enhanced cytotoxicity against multiple RMS cell lines in both two-dimensional culture and three-dimensional spheroid models. Furthermore, EGFR-CAR NK cells were highly efficient against chemotherapy-resistant RMS cells and patient-derived samples. Importantly, EGFR-CAR NK cells also exhibited improved tumor homing compared with non-transduced NK cells in an in vivo RMS xenograft model. Notably, the combination of EGFR-CAR NK cell therapy with fractionated radiotherapy further enhanced NK cell infiltration into the tumor and reduced tumor growth.

**Conclusion:** This study provides a proof-of-concept for EGFR-CAR NK cells as a promising immunotherapy for RMS, particularly when combined with radiotherapy to overcome barriers of solid tumors. This combinatorial approach may hold potential to improve outcomes for patients with RMS and other EGFR-expressing malignancies.

## BACKGROUND

Rhabdomyosarcoma (RMS) is the most common soft tissue malignancy in pediatric patients.[1] Overall survival of patients with

## WHAT IS ALREADY KNOWN ON THIS TOPIC

⇒ Despite a multimodal treatment regimen, outcomes for patients with rhabdomyosarcoma (RMS) are poor, and novel therapeutic strategies are urgently needed.

## WHAT THIS STUDY ADDS

⇒ Our study demonstrated the successful generation of epidermal growth factor receptor (EGFR)-targeting primary chimeric antigen receptor natural killer cells that efficiently eliminated RMS cells in vitro and inhibited the growth of RMS tumors in vivo when combined with radiotherapy.

## HOW THIS STUDY MIGHT AFFECT RESEARCH, PRACTICE OR POLICY

⇒ This study provides a promising basis for a novel treatment strategy for advanced RMS and possibly other malignancies with high medical need that are characterized by EGFR expression.

low-risk and localized disease has improved over the last decades with multimodal treatments, including surgical resection, chemotherapy, and radiotherapy. However, patients classified as high risk or those with metastatic or recurrent disease continue to have a poor prognosis, with a 5-year overall survival of less than 20%. In addition, one-third of all RMS patients with localized disease and two-thirds of those with metastatic disease experience relapse following first-line treatment, emphasizing the urgent need for novel therapeutic strategies.[2 3] Natural killer (NK) cells, which are innate lymphocytes and part of the immune system's first line of defense, have emerged as a promising alternative for cell-based immunotherapy.[4] Unlike T cells, NK cells can eliminate virus-infected or malignant cells without the need for prior antigen priming. By integrating activating and inhibitory signals of their broad receptor repertoire,

NK cells can also compensate for major histocompatibility complex-I loss in target cells, which is a major hurdle for T-cell therapies.[5 6]

Synthetic chimeric antigen receptors (CARs) can be incorporated to further enhance the potential of NK cell therapy and enable specific targeting to the tumor site. Early phase clinical trials have shown that CAR NK cell administration is feasible and safe, with high functionality and long-term persistence without evidence of side effects often associated with CAR T-cell therapies (NCT03056339).[7 8] However, targeting solid tumors remains challenging due to tumor antigen heterogeneity, low immune cell infiltration into the tumor tissue, and the immunosuppressive tumor microenvironment (TME).[9 10]

Epidermal growth factor receptor (EGFR) is a member of the EGFR/ErbB family of receptor tyrosine kinases and is frequently mutated or overexpressed in different cancers, including RMS, non-small cell lung cancer, and glioblastoma.[11 12] EGFR activity is more pronounced in a subset of RMS cells that are drug-resistant and likely to relapse.[13 14] Immunotoxins targeting EGFR have shown promise in reducing RMS tumor growth, suggesting that an approach directing cellular cytotoxicity to RMS cells via an EGFR-CAR may hold significant therapeutic potential.[15] Up to date, no clinical study has evaluated the potential of EGFR-targeted CAR NK cells against solid cancers.

Using the unique advantages of NK cells targeting EGFR as a tumor-associated antigen, this translational study aimed to develop an innovative immunotherapeutic approach for RMS. While EGFR-CAR NK cells on their own displayed only limited infiltration into tumor tissue, this was markedly enhanced when combined with radiotherapy. Hence, these findings reveal a promising treatment strategy for targeted cellular immunotherapy in patients with RMS.

## MATERIAL AND METHODS
### NK cell isolation and cultivation
Peripheral blood mononuclear cells were isolated by density gradient centrifugation from buffy coats of healthy donors (German Red Cross Blood Donation Service Baden-Württemberg-Hessen, Frankfurt am Main, Germany) as described previously.[16] All donors provided written informed consent, and the study was conducted in accordance with the Declaration of Helsinki.

NK cells were enriched using the EasySep Human NK Cell Enrichment Kit (STEMCELL, Vancouver, Canada) according to the manufacturer's instructions and cultured in NK-MACS Medium (Miltenyi Biotec, Bergisch-Gladbach, Germany) supplemented with NK-MACS supplements, 5% human AB plasma, 100 U/mL penicillin, and 100 µg/mL streptomycin (further referred to as NK-MACS) as previously reported.[17] Interleukin (IL)-15 (Miltenyi Biotec) was added to NK cell cultures at 120 U/mL every 3–4 days. Purity of isolated NK cells was validated by flow cytometry using the BD FACSCelesta

instrument and the following antibodies: CD3-BUV395 (SK7), CD56-BV421 (NCAM16.2), CD45-BV510 (HI30), CD14-BV711 (M5E2) (all BD Biosciences, San Jose, California, USA), CD19-BB515 (HIB19) and CD16-PE (3G8) (both BioLegend, San Diego, California, USA).

### Lentiviral vector production and transduction of NK cells
The lentiviral transfer plasmid pS-225.28.z-IEW was designed as described previously.[18] Briefly, a single chain fragment variable domain encompassing the variable regions of heavy and light chains of the clinically approved monoclonal antibody cetuximab[19] was linked to a Myc-tag and a CD8α hinge region, followed by transmembrane and costimulatory domains of CD28 and a CD3ζ signaling moiety (figure 1A and online supplemental figure S1). RD114-pseudotyped vector particles were generated with a second-generation lentiviral system using polyethylene-imine transfection into Lenti-X-293T cells (Takara Bio, Shiga, Japan).

Transduction of NK cells was performed 2 days after NK cell isolation (figure 1B).[16] Briefly, NK cells were collected and seeded at a density of $2\times10^6$ cells/mL in 250 µL NK-MACS medium in a 48-well flat-bottom plate. Lentiviral particles and the transduction enhancer Vecto-fusin-1 (Miltenyi Biotec; final concentration: 10 µg/mL) were diluted in basal NK-MACS medium and combined in identical volumes. After incubation for 10 min at room temperature, 250 µL of the suspension was added to the seeded NK cells to obtain a final cell density of $1\times10^6$ cells/mL. IL-15 (120 IU/mL) was added to the culture, and spinfection was performed at 800×g for 1.5 hours at 32°C. Half of the medium was replaced 1 day post-transduction with fresh NK-MACS medium and the corresponding amount of IL-15. CAR NK cells were analyzed by flow cytometry on a BD FACSCelesta instrument using the following antibodies: CD3-BUV395 (SK7), CD56-BV786 (NCAM16.2), and CD16-PE-CF594 (3G8) (BD Biosciences) and enhanced green fluorescent protein (EGFP) for CAR detection (online supplemental figure S2). Detailed phenotypic characterization was conducted as described in online supplemental methods (online supplemental figure S3).

### Luminescent 2D cytotoxicity assay
The cytotoxic potential of NK cells was analyzed in two-dimensional (2D) cultures using a luminescent cytotoxicity assay with firefly luciferase-expressing RMS cell lines, generated and cultivated as described in detail in online supplemental methods. Tumor cells were seeded with 7,500 cells/well in 100 µL of medium in a 96-well white flat-bottom plate (Merck Millipore, Burlington, Massachusetts, USA). Subsequently, the culture medium was removed, and 100 µL of the NK cell suspension or NK-MACS medium as control was added. The cytotoxic activity of non-transduced (NT) NK or CAR NK cells was analyzed at effector-to-target (E:T) cell ratios of 1:1, 2.5:1, or 5:1. After 4 hours of co-incubation at 37°C, 20 µL of 3 mM in vivo-grade VivoGlo luciferin (Promega, Madison,
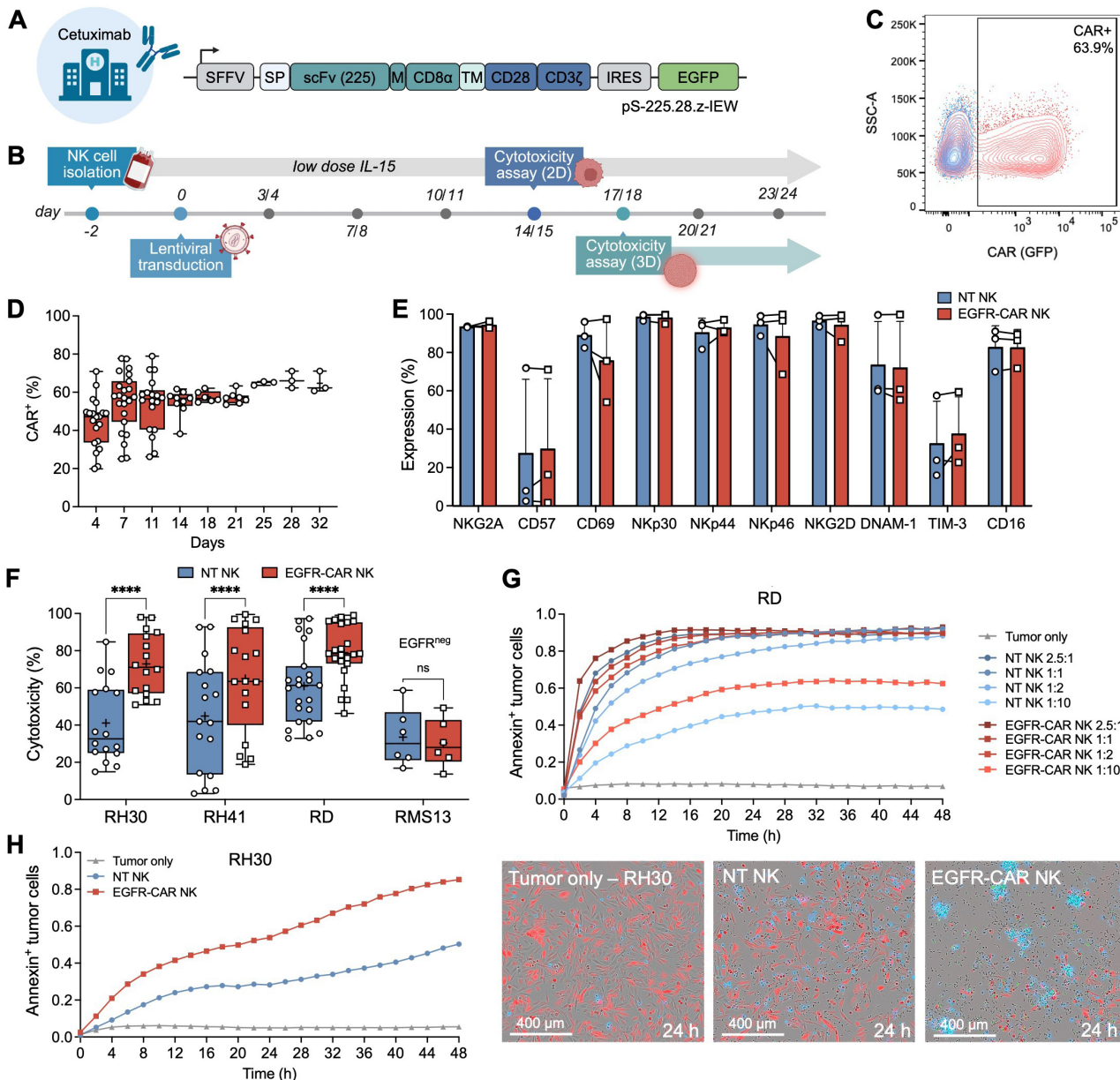
**Figure 1** EGFR-CAR NK cells efficiently eradicate EGFR-positive rhabdomyosarcoma (RMS) cells in vitro. (A) A construct encoding a second-generation CAR (225.28.z) was used for lentiviral transduction of NK cells. The CAR sequence under the control of the spleen focus forming virus (SFFV) promoter consists of an immunoglobulin heavy chain signal peptide (SP), a single chain fragment (scFv) based on the clinically used antibody cetuximab, a CD8α hinge region, followed by transmembrane (TM) and costimulatory domains of CD28 and a CD3ζ signaling domain. Enhanced green fluorescent protein (EGFP) linked via an internal ribosome entry site (IRES) was used as a marker for transgene expression. (B) Schematic of the CAR NK cell production workflow starting with primary NK cells from healthy donor buffy coats and subsequent lentiviral transduction. Cytotoxic activity of the generated CAR NK cells was assessed between days 14 and 24 post-transduction. (C) CAR expression was analyzed by flow cytometry using EGFP as a reporter gene (red). Non-transduced (NT) NK cells (blue) served as control. (D) CAR expression was detected in 50–60% of NK cells and remained stable for at least 30 days (n=3–23). (E) The receptor repertoire of primary NT (blue circles) and EGFR-CAR NK cells (red squares) was analyzed by flow cytometry (n=3). (F) Cytotoxic activity of expanded EGFR-CAR NK cells was investigated against alveolar (RH30, RH41) and embryonal (RD) RMS cell lines at an effector-to-target (E:T) ratio of 5:1 after 4 hours (n=16–23). EGFR-negative RMS cells (RMS13) served as control (n=6). The graphs show all individual data points, with the black middle line representing the median value, and the mean indicated by a plus (+) sign. Data were analyzed by two-way analysis of variance followed by Šídák's multiple comparison test. (G, H) Apoptosis induction by EGFR-CAR NK (red squares) compared with NT NK cells (blue circles) was analyzed via annexin V staining using the IncuCyte Live-Cell Analysis Platform at different E:T ratios ranging from 2.5:1 to 1:10. Data for one representative NK cell donor against the FP-RMS cell line RD (G) and the FN-RMS cell line RH30 (H, left panel) are shown. Images taken after 24 hours of co-incubation display remaining RH30 cells (red), NT NK cells (gray), EGFR-CAR NK cells (green) and apoptosis induction by annexin V staining (cyan) (H, right panel). CAR, chimeric antigen receptor; GFP, green fluorescent protein; IL, interleukin; NK, natural killer; RMS, rhabdomyosarcoma.

Wisconsin, USA) was added to each well, and samples were incubated for 15 min at 37°C. Luminescence was recorded using the GloMax Multi Detection Microplate Reader (Promega). All conditions were measured in triplicates. To determine maximum lysis, 10% Triton-X 100 in NK-MACS was added during co-incubation. To calculate specific cytotoxicity, spontaneous lysis was subtracted from experimental values, and subsequently the following formula was used:

$$\text{Cytotoxicity (\%)} = 100 - \left( \frac{\text{Co-culture}}{\text{Tumor only}} \times 100 \right)$$

Additional information on the chemoresistant RMS cell lines and primary patient-derived RMS cells used is provided in online supplemental methods.

### IncuCyte-based 2D apoptosis assay
Induction of apoptosis in RMS cell lines by EGFR-CAR or NT NK cells was analyzed in a 2D assay using the IncuCyte SX5 Live-Cell Analysis Platform (Sartorius, Goettingen, Germany) with a green/orange/near-infrared (NIR) optical module. $1 \times 10^4$ mCherry/luc-expressing RMS cells were seeded in 100 µL of culture medium in a 96-well clear flat-bottom plate and allowed to attach for 1–2 hours at 37°C. The medium was aspirated and replaced with NK-MACS medium (tumor only), or suspensions of NT or EGFR-CAR NK cells at different E:T ratios. Immediately after effector cell addition, IncuCyte Annexin V NIR dye (Sartorius) was added at a final dilution of 1:400 in NK-MACS medium containing 1 mM $CaCl_2$. Images were captured every 2 hours at 10× magnification. The fraction of annexin-positive tumor cells was quantified by dividing the overlap of the mCherry and NIR signals by the total mCherry signal.

### IncuCyte-based 3D cytotoxicity assay
Long-term cytotoxicity of NK cells was assessed with three-dimensional (3D) tumor spheroids using either the Incu-Cyte S3 or SX5 live-cell analysis platforms. RMS cells were seeded at a density of $1 \times 10^4$ cells in 200 µL per well in a 96-well flat-bottom ultra-low-attachment plate (Corning, Corning, New York, USA). Cells were then centrifuged for 10 min at 1,000×g and allowed to grow for 4 days. On day 3 after seeding, half of the medium was replaced with fresh culture medium.

On day 4, again half of the medium was removed, and $5 \times 10^4$ NK cells or NK-MACS medium as a control were added to the respective wells. All conditions were measured in triplicates. To analyze spheroid growth, phase contrast and red fluorescence images were captured every 4 hours for 4 days at 4× magnification. The Brightfield Object Red Integrated Intensity (RFU × µm²/ image) was assessed using the IncuCyte 2023A software.

Spheroid growth (%) was determined using the following formula:

$$\text{spheroid growth (\%)} = 100 \times \frac{(\text{value-baseline (0 hours)})}{\text{baseline (0 hours)}}$$

The area under the curve was calculated for each individual NK cell donor and condition. The arithmetic means for each condition were compared and tested for statistical significance using repeated measures (RM) one-way analysis of variance, followed by Tukey's multiple comparison test.

### In vivo RMS xenograft model
All animal experiments were approved by Regierungspräsidium Darmstadt (approval number FK/2011) and conducted in accordance with the requirements of the German Animal Welfare Act. NOD.Cg-*Prkdc^scid^Il2rg^tm1Wjl^*/ SzJ (NSG) mice were injected subcutaneously (s.c.) with $0.1 \times 10^6$ RD-GFP/luc cells. Tumor growth was monitored by caliper measurements and bioluminescence imaging (BLI) using the IVIS Lumina II platform (Revvity Health Sciences, Lawrence, Massachusetts, USA), as described previously.[20]

### Non-invasive imaging of NK cell homing
To analyze the migratory potential of NK cells in vivo, NK cells were stained with XenoLight DiR dye (Revvity Health Sciences) according to the manufacturer's instructions. Labeled NK cells were resuspended in phosphate-buffered saline (PBS) at a density of $10 \times 10^6$ cells/100 µL for intravenous (i.v.) injection into the tail vein of 8–12 weeks old female NSG mice on day 40 after tumor engraftment. Control animals received PBS. In vivo homing of labeled NK cells was measured on days 1, 2, and 5 after administration using fluorescence imaging with the IVIS platform. Mouse spleen and tumor samples were collected and preserved in ROTI Histofix 4% formaldehyde (Carl Roth, Karlsruhe, Germany) for histochemical analysis. A similar experiment was performed with 23 weeks old male NSG mice, and an additional experimental group receiving fractionated radiation (see below) in combination with EGFR-CAR NK cells was included. To determine NK cell migration regarding tumor size, the following formula was used:

$$\text{Tumor specific NK cell migration} = \frac{\text{NK cell fluorescene}}{\text{tumor bioluminescence}} \times 10^5$$

### Combination of CAR NK cells and radiotherapy
7–10 weeks old female NSG mice s.c. injected with RD cells were distributed into the following treatment groups on day 25 after tumor engraftment and visual detection of tumor nodules: untreated mice (n=6), radiotherapy (n=6), radiotherapy+NT NK cell injections (n=6), or radiotherapy+EGFR CAR NK cell injections (n=6).

Mice treated with image-guided radiation therapy received fractionated single doses of 2.5 Gy applied four times a week until reaching a total dose of 25 Gy. Animals were immobilized with 2.5% isoflurane anesthesia (AbbVie, Wiesbaden, Germany) and subjected to an on-board Cone-Beam CT (CB-CT) operated at 60 kV, 0.8 mA using a Small Animal Radiation Research Platform (SARRP, X-strahl, Camberley, UK). The CB-CT image data were then transferred to MuriPlan Software (X-strahl) for contouring, and individual isocenters were selected for

targeted radiation therapy by applying a two-field geometry with either 5×5 mm or 10×10 mm collimated beams operating at 220 kV and 13 mA at a dose rate of 5.2 cGy/s.

$10×10^6$ NK cells were injected i.v. four times starting on day 2 after the last radiation dose, with a minimum gap of 3 days between each dosage. To allow NK cell persistence, IL-2 was administered daily at 25 000 IU/mL in 50 µL s.c. for 4 weeks. Mice were sacrificed on reaching a predefined termination criterion, and spleen and tumor samples were collected for immunofluorescence microscopy analysis (see online supplemental methods). The sample identity was blinded to the executors of the consecutive analyses.

For cryopreservation, NK cells were frozen in Roswell Park Memorial Institute 1640 medium supplemented with 20% fetal bovine serum and 10% dimethyl sulfoxide 11 days post-transduction. Cells were then gently thawed and cultivated 5 days prior to in vivo administration.

### Data analysis and statistics
Graphical representation of the data and statistical analyses were performed using GraphPad Prism V.10.0, assuming normal distribution of NK cell function in healthy donors. Only data from experiments with three or more biological replicates (n≥3) were considered for statistical analysis. All results are presented as mean±SD unless stated otherwise. Differences with p values *p<0.05, **p<0.01, ***p<0.001, and ****p<0.0001 were considered statistically significant.

## RESULTS
### Engineering of NK cells with a cetuximab-based EGFR-CAR allows precision targeting of rhabdomyosarcoma
Primary human NK cells were modified by lentiviral transduction to express an EGFR-directed second-generation CAR,[18] followed by an expansion period in the presence of low-dose IL-15 (figure 1A,B). Two times a week, CAR expression was determined by quantification of EGFP, linked as a marker to the CAR sequence via an internal ribosome entry site (figure 1C). Interestingly, the proportion of CAR-expressing cells increased during NK cell expansion from 44.1%±13.1% on day 4 to 54.8%±6.9% on day 14, and 57.1%±3.2% on day 21 post-transduction (figure 1D). The phenotypic profiles of NT and CAR NK cells were analyzed by flow cytometry on day 14 post-transduction, which revealed no differences in the activating receptors NKp30, NKp44, NKp46, NKG2D, and DNAM-1 (figure 1E). Likewise, expression levels of the activation markers CD57 and CD69, the inhibitory receptors NKG2A and TIM-3, and the maturation marker CD16 were equivalent in NT and CAR NK cells.

Next, the cytotoxic capacity of EGFR-CAR NK cells was analyzed with a broad range of RMS target cell lines, including the fusion-negative (FN-RMS) and the more aggressive fusion-positive subtype (FP-RMS), characterized by translocation of forkhead box O1 (*FOXO1*) and fusion to either paired box 3 (*PAX3*) or *PAX7*

(figure 1F).[21] Thereby, a significantly increased cytotoxicity of 72.9% over 41.1% for RH30 and 65.0% over 44.9% for RH41 cells (both FP-RMS) was observed with EGFR-CAR NK cells compared with NT NK cells after only 4 hours of co-incubation at an E:T ratio of 5:1 (figure 1F). The FN-RMS cell line RD showed increased EGFR-CAR NK-mediated cytotoxicity of 78.9% over NT NK cells with 61.0%. As expected, no significant difference in cytotoxicity of CAR NK and NT NK cells against the FP-RMS cell line RMS13 was observed, which does not express the CAR target antigen EGFR and served as a control (figure 1F). Enhanced killing of EGFR-positive targets by CAR NK cells, compared with NT NK cells, was confirmed by accelerated apoptosis induction in the RD cell line observed across all analyzed E:T ratios, ranging from 2.5:1 to 1:10. This was measured by annexin V staining during live-cell imaging for up to 48 hours (figure 1G). Notably, similar results were obtained for more NK-resistant RH30 cells (figure 1H, left panel). After 24 hours, only a small proportion of RH30 cells (red) remained alive in the co-incubation setting (figure 1H, right panel, online supplemental videos 1-3).

In summary, this comprehensive phenotypical and functional assessment revealed strong transgene expression of EGFR-CAR NK cells, which exhibited significantly enhanced in vitro antitumor efficacy against RMS.

### EGFR-CAR NK cells retain high antitumor activity at low effector-to-target cell ratios and in 3D RMS spheroid models
To evaluate cell killing activity of the CAR NK cells at lower, clinically more relevant E:T ratios, and to determine potential effects of the antigen dose, including the minimum antigen threshold required for activity, additional cytotoxicity assays were performed in 2D cell cultures. EGFR expression was analyzed in all RMS cell lines, with low and medium EGFR expression determined for RH41 (geometric mean fluorescence intensity, MFI: 196) and RH30 (MFI: 681), and high expression for RD (MFI: 1826). The RMS13 cell line served as a control for RMS-directed natural cytotoxicity of CAR NK and NT NK cells due to its lack of EGFR expression (figure 2A). A significant increase in cytotoxicity was observed for EGFR-CAR NK cells against all tested EGFR-expressing RMS cell lines at the highest E:T ratio of 5:1 (figure 2B). At the lower E:T ratios of 2.5:1 and 1:1, superior efficacy of EGFR-CAR NK cells was still found for the FN-RMS cell line RD and the FP-RMS cell line RH30.

Next, the cytotoxic activity of EGFR-CAR NK cells was evaluated using 3D RMS spheroids, which serve as a suitable in vitro model for solid tumor structures. Spheroids were exposed to either EGFR-CAR or NT NK cells for 4 days, with consecutive images captured at 4-hour intervals (figure 2C,D, online supplemental figure S4). Notably, NT NK cells already suppressed tumor growth of all examined RMS spheroids, with complete elimination of RH41 spheroids observed at later time points (84–96 hours). Nevertheless, compared with NT NK cells, target cell killing by EGFR-CAR NK cells was more efficacious in the
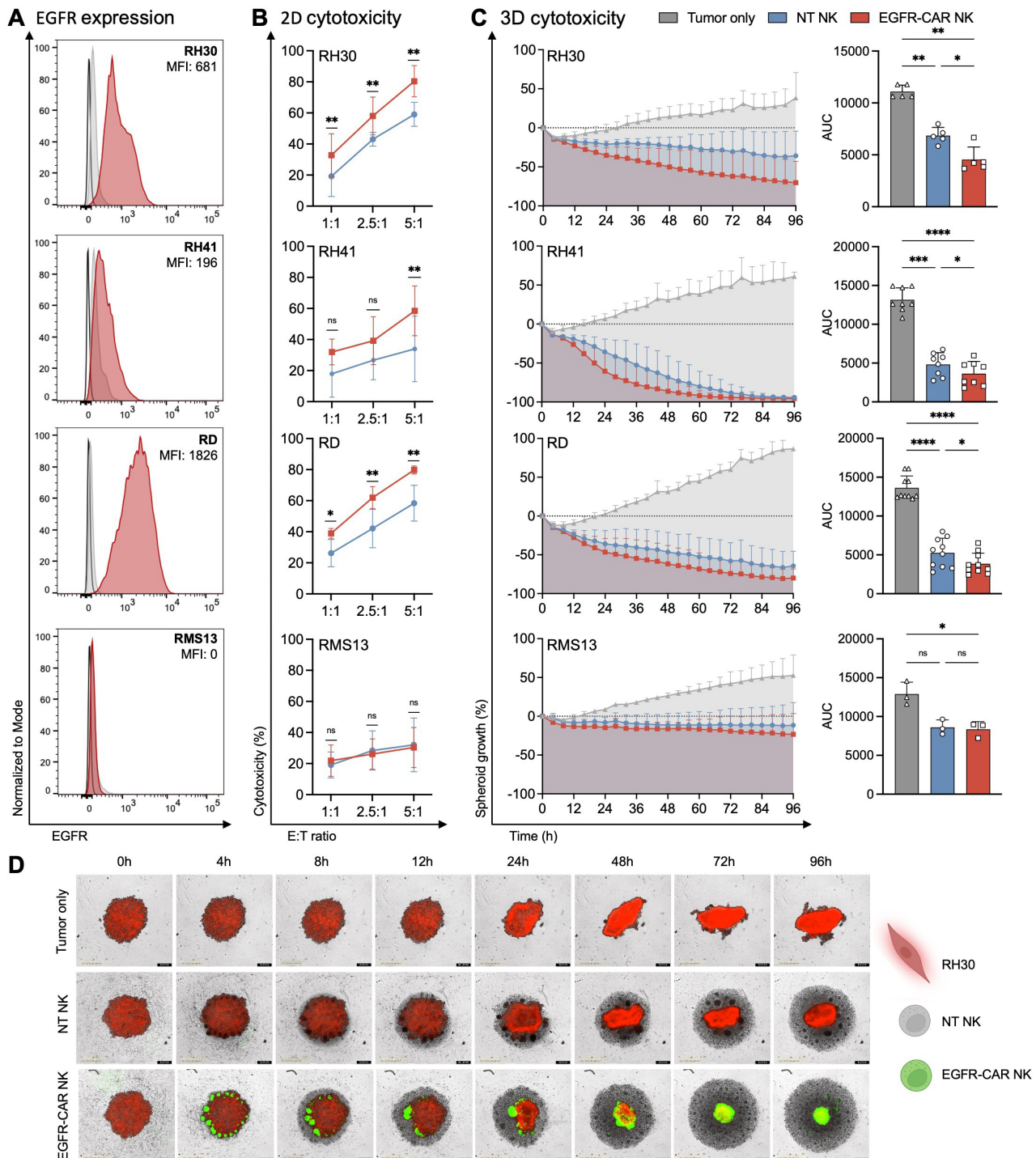
**Figure 2** EGFR-CAR NK cells display high antitumor activity at low effector-to-target cell ratios and in 3D RMS spheroid models. (A) EGFR surface expression was analyzed by flow cytometry on four RMS cell lines (RH30, RH41, RD, RMS13). MFI values indicate relative EGFR expression levels. The EGFR-negative RMS cell line RMS13 served as a control. (B) Cytotoxic activity of NT NK (blue circles) and EGFR-CAR NK cells (red squares) was assessed after 4 hours of co-cultivation at different effector-to-target (E:T) cell ratios (1:1, 2.5:1, 5:1) against the fusion-positive-RMS cell lines RH30 and RH41 and the fusion-negative-RMS cell line RD (n=4–6) using a luciferase-based assay. EGFR-negative RMS13 cells were included to assess CAR-independent natural cytotoxicity. Data were analyzed by two-way ANOVA followed by Šídák's multiple comparisons test. (C) Eradication of RMS spheroids by EGFR-CAR NK (red squares) compared with NT NK cells (blue circles) was monitored over time by live-cell imaging using the IncuCyte platform for up to 96 hours at an E:T ratio of 1:1. AUC measurements were used to quantify NK cell cytotoxicity against RMS spheroids (n=3–10). Data were analyzed using repeated measures one-way ANOVA followed by Holm-Šídák's multiple comparisons test. (D) Representative time-lapse images of RH30 spheroids (red) in combination with NT NK cells (gray) or EGFR-CAR NK cells (green). ANOVA, analysis of variance; AUC, area under the curve; CAR, chimeric antigen receptor; EGFR, epidermal growth factor receptor; MFI, geometric mean fluorescence intensity ;NK, natural killer; NT, non-transduced; RMS, rhabdomyosarcoma; 2D, two-dimensional; 3D, three-dimensional.
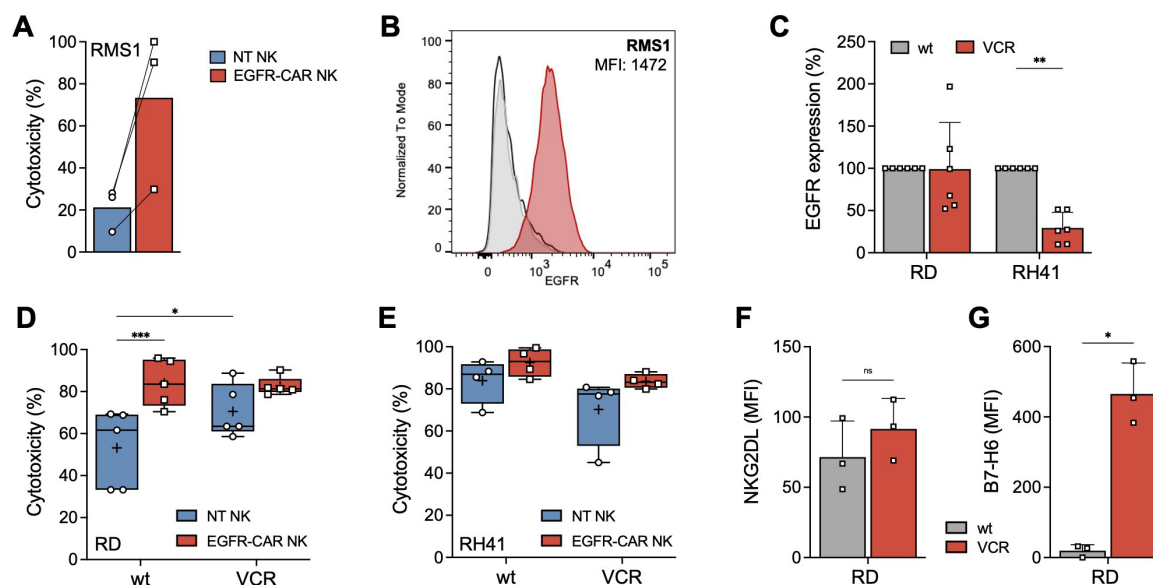
**Figure 3** EGFR-targeted CAR NK cells demonstrate effectiveness against patient-derived primary RMS and chemotherapy-resistant RMS cell lines. (A) Activity of EGFR-CAR NK cells (red squares) and NT NK cells (blue circles) against a primary FP-RMS cell isolate (RMS1) derived from a patient with progressive disease was compared after 4 hours of co-incubation (E:T ratio 5:1, n=3). Data were analyzed by paired t-test. Only statistically significant comparisons are indicated. (B) EGFR expression by RMS1 cells was assessed by flow cytometry (n=3). One representative measurement is shown. (C) EGFR expression by parental and VCR-resistant RMS cell lines RD and RH41 was determined using flow cytometry. EGFR expression by VCR-resistant cell lines is indicated relative to the corresponding parental cell lines (100%). Results were analyzed using two-way ANOVA followed by Šídák's multiple comparison test. (D, E) Cytotoxic activity of EGFR-CAR NK cells (red squares) and NT NK cells (blue circles) against the parental (wt) FN-RMS cell line RD (D), the FP-RMS cell line RH41 (E) and the corresponding VCR-resistant variants was investigated in 4-hour cytotoxicity assays at an E:T ratio of 5:1. Data were analyzed using two-way ANOVA followed by Fisher's LSD test (n=4–5). All individual data points, as well as minimum and maximum values are shown. The black-centered line represents the median. The mean is indicated by a plus (+) sign. Only statistically significant differences are indicated. (F, G) Expression of NKG2DL and B7-H6 by parental and VCR-resistant cell lines was analyzed by flow cytometry (n=3). Results are indicated as MFI and were analyzed using a paired t-test. ANOVA, analysis of variance; CAR, chimeric antigen receptor; EGFR, epidermal growth factor receptor; E:T, effector-to-target; FN, fusion-negative; FP, fusion-positive; LSD, least significant difference; NK, natural killer; NKG2DL, NKG2D ligands; NT, non-transduced; MFI, geometric mean fluorescence intensity; RMS, rhabdomyosarcoma; VCR, vincristine; wt, wildtype.

case of RH30, RH41, and RD spheroids, illustrated by the differences in the area under the curve. NT NK cells were unable to achieve comparable efficacy against RH30 and RD spheroids, even after extended co-incubation. Importantly, the natural cytotoxicity of EGFR-CAR NK cells remained unaffected by CAR expression, as evidenced by the comparable activity of EGFR-CAR and NT NK cells against EGFR-negative RMS13 spheroids.

Taken together, these data confirm robust antitumor activity of EGFR-CAR NK cells also against 3D RMS spheroids, underscoring their potential to attack solid tumor structures.

### EGFR-targeted CAR NK cells are active against patient-derived primary RMS cells and chemotherapy-resistant RMS cell lines

To investigate the effectiveness of EGFR-CAR NK cells against patient-derived primary RMS cells, we performed short-term cytotoxicity assays using an FP-RMS specimen from a pediatric patient with progressive disease following chemotherapy and surgical resection of the primary tumor, referred to as RMS1. After a 4-hour co-incubation at an E:T ratio of 5:1, EGFR-CAR NK cells demonstrated superior ability to eliminate RMS1 cells when compared

with NT NK cells (p=0.0723) (figure 3A), facilitated by expression of the EGFR target antigen by the RMS1 cells (figure 3B).

Despite the well-known chemosensitivity of RMS, many patients relapse after standard therapy, representing a patient cohort with poor prognosis and worse outcomes. Therefore, in the next set of experiments, we analyzed whether chemotherapy-resistant RMS cells are still sensitive to adoptive EGFR-CAR NK cell therapy. Chemotherapy-resistant sublines were generated by continuous exposure of the parental FN-RMS RD and FP-RMS RH41 cell lines to vincristine (VCR) (see online supplemental methods). EGFR expression in the VCR-resistant RD subline was not altered. In contrast, VCR-resistant RH41 cells showed reduced expression of EGFR (figure 3C). EGFR-CAR NK cells displayed similarly high activity against parental and VCR-resistant RD cells. While increased cytotoxicity was observed for NT NK cells against the VCR-resistant cells, this activity did not reach the level of CAR NK cells (figure 3D). Interestingly, despite reduced target antigen expression in VCR-resistant RH41 cells, EGFR-CAR NK cells maintained

similar killing efficacy as against the parental RMS cell line (figure 3E). Altered NK cell ligand expression on continuous VCR treatment was analyzed for individual activating ligands on RD (figure 3F,G) and RH41 cells (online supplemental figure S5). VCR-resistant RD cells displayed significantly enhanced expression of B7-H6, a main ligand of the activating receptor NKp30 on NK cells. The expression of ligands for the activating receptor NKG2D (NKG2DL) was not significantly altered on VCR exposure in RD cells. However, NKG2DL was highly upregulated on VCR-resistant RH41 cells compared with the parental cell line (online supplemental figure S5).

These findings demonstrate that EGFR-CAR NK cells retain potent cytotoxic activity against both parental and VCR-resistant RMS cells, highlighting their potential as an effective therapeutic option for chemotherapy-resistant RMS.

### EGFR-CAR NK cells demonstrate tumor homing in NSG mice

To validate the promising in vitro findings and investigate the antitumor activity of EGFR-CAR NK cells in a more physiological setting, a recently reported NSG RMS xenograft model was used.[20] In brief, NSG mice were inoculated s.c. with luciferase-expressing RD cells, and successful tumor cell engraftment was confirmed by BLI (figure 4A). Afterwards, $10 \times 10^6$ NK cells were fluorescently labeled and injected intravenously as a single dose into the tumor-bearing animals. Localization of the tumors was confirmed by BLI, and NK cell trafficking was monitored over a time course of 120 hours by fluorescence measurements in anesthetized mice (figure 4B). Both EGFR-CAR and NT NK cells were detected after 24, 48, and 120 hours at the tumor site and in other NK cell-homing organs, including lungs, liver and spleen.
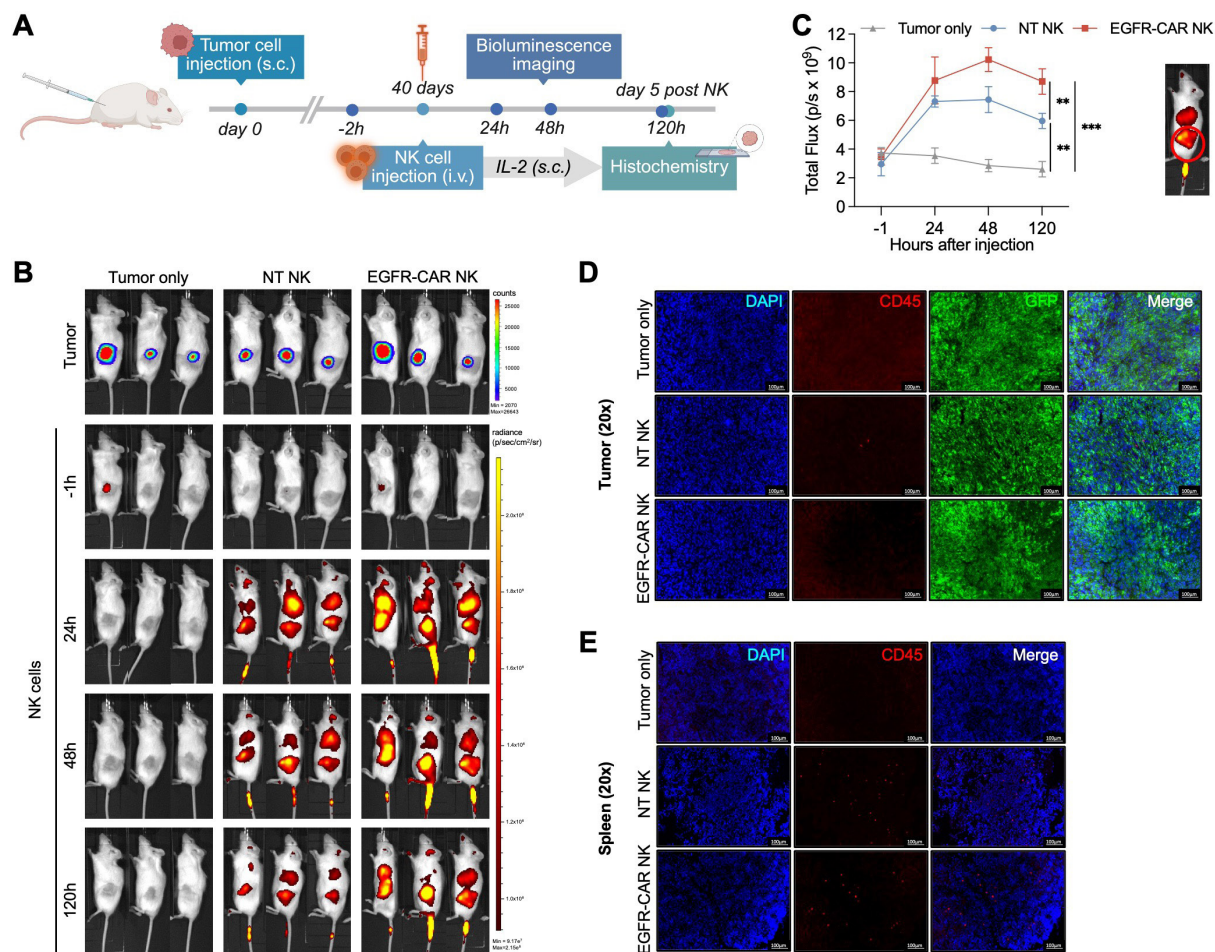


**Figure 4** EGFR-CAR NK cells home to established RMS tumor xenografts in NSG mice. (A) Pre-labeled EGFR-CAR or NT NK cells were ii.v injected into s.c RMS tumor-engrafted mice 40 days post tumor implantation, and in vivo homing was analyzed for 5 days. (B) Tumor growth was assessed by bioluminescence imaging (top row). NK cell migration was analyzed using fluorescence imaging (bottom rows) at different time points after NK cell injection: 24, 48 and 120 hours. Unspecific fluorescence signal was quantified 1 hour before NK cell administration. (C) NK cell trafficking to the tumor site and persistence was quantified over the 5 days observation period and analyzed by two-way ANOVA followed by Holm–Šídák's multiple comparisons test (n=3). (D) Immunofluorescence analysis of tumor sections was performed to assess infiltration of NK cells (CD45, red) deep into the tumor (GFP, green) tissue. (E) Spleen sections were analyzed for comparison. ANOVA, analysis of variance; CAR, chimeric antigen receptor; EGFR, epidermal growth factor receptor; IL, interleukin; i.v., intravenous; NK, natural killer; NT, non-transduced; RMS, rhabdomyosarcoma; s.c., subcutaneous.

Notably, quantification of fluorescence signals in the tumor area revealed a significantly enhanced migration of EGFR-CAR NK cells to the tumor when compared with NT NK cells (figure 4C). Nevertheless, immunofluorescence analysis of tissue sections did not confirm immune cell infiltration deep into the tumor mass (figure 4D), while NK cells were readily detected in the spleens of NT and EGFR-CAR NK-treated mice (figure 4E). In line with these results, treatment of mice with three consecutive injections of $10 \times 10^6$ EGFR-CAR or NT NK cells on days 7, 11 and 14 following tumor inoculation did not lead to significantly delayed tumor growth (online supplemental figure S6).

Collectively, these data suggest that despite initial immune cell migration to the tumor site, tumor infiltration was inefficient in this setting and did not translate into a therapeutic effect.

### Radiotherapy augments NK cell-mediated cytotoxicity in rhabdomyosarcoma

Next, it was investigated whether radiotherapy could synergize with EGFR-CAR NK cell therapy to improve antitumor responses in RMS. Radiotherapy is known to lead to the formation of reactive oxygen species and thus directly damage tumor cells by inducing DNA double-strand breaks. In addition, radiotherapy can alter the TME and indirectly induce antitumor effects in an immunocompetent host by priming the immune response and enhancing immune cell infiltration.

First, to evaluate the effect of radiotherapy on NK cell-mediated cytotoxicity against RMS in vitro, live-cell imaging assays were performed using both monolayer and 3D spheroid cultures (figure 5A,B). RMS cells were irradiated with 25 Gy 1-day prior to co-incubation with EGFR-CAR or NT-NK cells at an E:T ratio of 1:10 (figure 5A). Radiotherapy enhanced NK cell-mediated cytotoxicity, with EGFR-CAR NK cells showing superior tumor cell clearance compared with NT NK cells (figure 5C). Notably, radiotherapy alone significantly reduced tumor growth. Consistent effects were observed in RMS spheroid models, where irradiated spheroids exhibited increased susceptibility to NK cell attack, particularly by EGFR-CAR NK cells, across three independent donors (figure 5D). To investigate treatment-induced modulation of the TME, chemokine levels were quantified post-radiotherapy, NK cell treatment, or a combination of both (figure 5E,F, online supplemental figures 8; 9). Irradiation significantly increased IL-8 (C-X-C motif chemokine ligand 8, CXCL-8) concentrations in both culture models, while C-C motif chemokine ligand 2 (CCL2) was upregulated in all NK cell-treated conditions. The effects of radiotherapy on NK cell migration were subsequently examined in RMS-bearing mice (figure 5G). NK cell infiltration data shown in figures 4B and 5G were combined and normalized to the respective tumor-bearing control mice for comparative analysis. A trend toward increased NK cell presence at the tumor site was observed 24 hours post-injection in irradiated animals (figure 5H). To

account for radiotherapy-induced tumor shrinkage, NK cell signals (figure 5G) were normalized to the individual tumor burden of each mouse, revealing enhanced NK cell accumulation in the radiotherapy and EGFR-CAR NK cell combination group (figure 5I). Despite this increase in early infiltration, only low NK cell numbers were detected in tumor sections 5 days after their application (online supplemental figure S10E–H), although high NK cell numbers were present in the spleens (online supplemental figure S10A–D). EGFR expression in tumor tissues remained consistent across all treatment groups and control animals (online supplemental figure S11A,B). Collectively, these data demonstrate that radiotherapy enhances the tumor infiltration of adoptively transferred NK cells in RMS, particularly when combined with EGFR-CAR NK cells.

### Combining radiotherapy with EGFR-CAR NK cells enhances their therapeutic efficacy in vivo

To further explore the therapeutic potential of this combination strategy in vivo, the antitumor effects of EGFR-CAR NK cells following local irradiation were examined in RMS-bearing mice. Accordingly, NSG mice were inoculated s.c. with RD cells, and after visual confirmation of tumor formation, the animals were treated with fractionated radiation at the tumor site, as previously described (figure 6A).[20] Mice receiving 10 single doses of 2.5 Gy (Σ 25 Gy) image-guided radiation therapy showed significantly delayed tumor growth when compared with untreated control animals, becoming visible after four doses of radiation (figure 6B). 2 days after the final radiation treatment, adoptive NK cell therapy was initiated in two experimental groups with intravenous administration of four doses of EGFR-CAR or NT NK cells. A transient reduction in absolute tumor size was achieved after the fourth treatment, and overall, a further delayed tumor growth when compared with radiotherapy alone (figure 6B). Of note, in this experiment, the first three NK cell treatments consisted of cryopreserved NT NK or CAR NK cell preparations, followed by a freshly prepared NK cell product. Thereby, CAR expression as well as cytotoxic function against RD monolayers was comparable irrespective of prior cryopreservation or direct administration of the NK cells (online supplemental figure S7). Quantification of the area under the curve confirmed that radiation therapy alone, as well as combination with NT NK or CAR NK cells, all resulted in a significant reduction in tumor growth compared with untreated control animals (figure 6C,D). Importantly, radiotherapy in combination with EGFR-CAR NK cells proved superior to combination with NT NK cells or radiotherapy alone, which became apparent at later time points (figure 6E). As endpoint analysis, final tumor volumes were analyzed for all experimental groups (figure 6F), with the smallest tumor nodules found in radiotherapy-treated mice that had in addition received EGFR-CAR NK cells. In contrast, the largest tumor nodules were observed in untreated control mice, with one-third of the animals exhibiting tumors
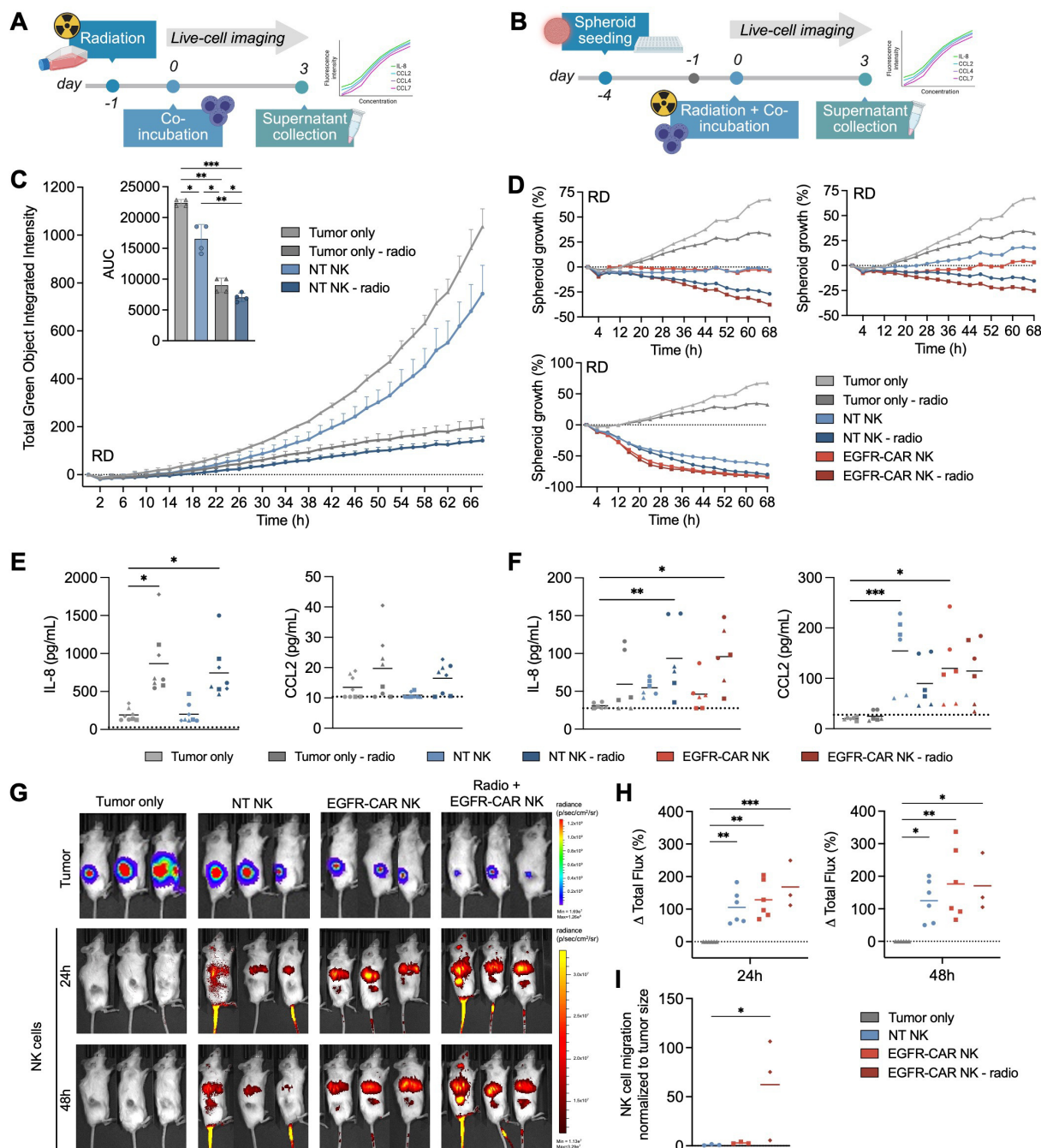
**Figure 5** Radiation enhances chemokine secretion and NK cell-mediated tumor control in r RMS models. (A, B) Experimental timeline for co-culture of irradiated RD cells with NT NK cells in 2D monolayer (A) or 3D spheroid assays (B). (C) Tumor growth over time after exposure to radiation, co-incubation with NT NK cells (E:T ratio of 1:10) or a combination analyzed by live cell imaging in 2D monolayer culture (n=4). AUC measurements were used to quantify NK cell cytotoxicity and data were analyzed using repeated measures one-way ANOVA followed by Holm-Šídák's multiple comparisons test. (D) Spheroid growth upon irradiation, NT or EGFR-CAR NK cell treatment and combinatorial regimens was assessed for 68 hours (three individual NK donors, E:T ratio 1:1). (E, F) Quantification of IL-8 and CCL2 levels in supernatants from 2D (E) and 3D (F) assays. Samples were measured in duplicates and biological replicates are indicated by different symbols. Data were analyzed using Friedman's test followed by Dunn's multiple comparison test. (G) In vivo BLI of tumor-bearing mice at 0, 24 and 48 hours post-treatment. NK cell migration was analyzed by fluorescence imaging. (H) NK cell trafficking to the tumor site was quantified at 24 and 48 hours and normalized to control mice (tumor only). The mean total flux of all replicates analyzed from figures 5G and 4B is indicated. Data were analyzed using ordinary one-way ANOVA followed by Holm-Šídák's multiple comparisons test (n=3–6). (I) NK cell fluorescence values 24 hours after NK cell application (G) were normalized to the tumor signals quantified by BLI for each group and analyzed by Kruskal-Wallis test followed by Dunn's multiple comparisons test (n=3 per group). ANOVA, analysis of variance; AUC, area under the curve; BLI, bioluminescence imaging; CAR, chimeric antigen receptor; CCL2, C-C motif chemokine ligand 2; EGFR, epidermal growth factor receptor; E:T, effector-to-target; IL, interleukin; NK, natural killer; NT, non-transduced; 2D, two-dimensional; 3D, three-dimensional.
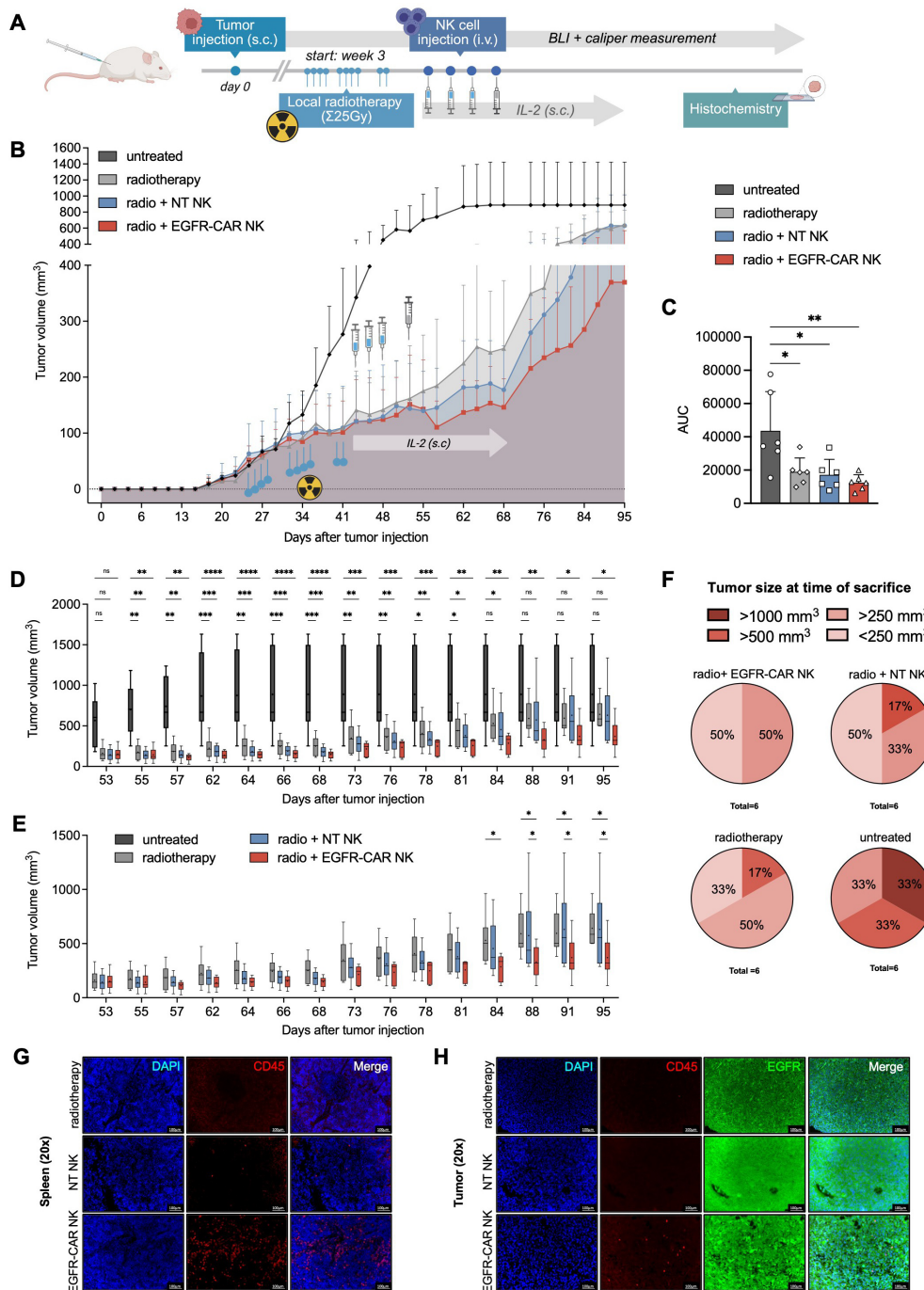
**Figure 6** Combination of radiotherapy and adoptive EGFR-CAR NK cell therapy inhibits RMS tumor growth in vivo. (A) Experimental design: RMS tumors were established by s.c. injection of RD cells followed by fractionated radiation (10×2.5 Gy). Four consecutive doses of either cryopreserved (blue syringe) or freshly prepared (gray syringe) EGFR-CAR or NT NK cells were administered i.v. as indicated. (B) Tumor growth was assessed by caliper measurements for each treatment group (n=6): untreated mice (dark gray), radiotherapy (light gray), radiotherapy+NT NK (blue) and radiotherapy+EGFR CAR NK cells (red). (C) The AUC was calculated to determine treatment effects over time. Data were analyzed using one-way ANOVA followed by Holm-Šídák's multiple comparisons test (n=6). Only statistically significant differences are indicated. (D, E) Tumor progression was compared between each treatment group after the last NK cell administration on day 53 to investigate the contribution of NK cell therapy after radiation. Data were analyzed by two-way ANOVA followed by Holm-Šídák's multiple comparison test. Minimum and maximum values are shown. The black centered line indicates the median. The mean is represented by a plus (+) sign. Only statistically significant differences are indicated. (F) Final tumor sizes were assessed during endpoint analysis at the time of sacrifice and grouped into four categories as indicated. (G, H) Immunofluorescence analysis of spleen (G) and tumor sections (H) from one representative animal of each treatment group. Nuclei/DAPI (blue), CD45 (red), EGFR (green). ANOVA, analysis of variance; AUC, area under the curve; BLI, bioluminescence imaging; CAR, chimeric antigen receptor; DAPI, 4′,6-diamidino-2-phenylindole; EGFR, epidermal growth factor receptor; IL, interleukin; i.v., intravenous; NK, natural killer; NT, non-transduced; RMS, rhabdomyosarcoma; s.c., subcutaneous.

>1,000 mm³. Immunofluorescence analysis of spleens and tumor sections obtained 28 days after the final NK cell administration confirmed persistence of both NT and EGFR-CAR NK cells in the spleens (figure 6G), whereas only in EGFR-CAR NK cell-treated mice NK cells were also detected in the tumors. High EGFR expression was retained in the analyzed tumor sections of each treatment group (figure 6H).

Taken together, these data demonstrate that the combination of radiotherapy with EGFR-targeted CAR NK cells facilitates tumor infiltration by the effector cells, resulting in more effective inhibition of RMS tumor growth than radiation treatment alone.

## DISCUSSION

The prognosis of patients with RMS remains poor after exhaustion of conventional therapy consisting of resection, local radiation, and poly-pragmatic chemotherapy.[22 23] 5-year survival rates of less than 20% have been reported for relapsed or high-risk RMS.[24 25] Successful treatment of hematological malignancies with CAR-engineered NK cells encourages their development also as a therapeutic strategy for solid tumors.[5 7] Here, a potential role for CAR NK cell therapy in RMS was identified, and, to the best of our knowledge, the first report on the use of primary EGFR-targeted CAR NK cells in combination with radiotherapy was presented. While the US Clinical Trials Registry (ClinicalTrials.gov) currently lists 25 clinical trials that investigate CAR NK cells from different sources for the treatment of various solid tumors, none of them explores EGFR-targeted CAR NK cells. Six clinical trials specifically addressed adoptive NK cell therapy for RMS, but without CAR modification of the effector cells,[26] and the benefit of preoperative or postoperative radiotherapy for patients with RMS is currently evaluated in the Frontline and Relapsed RMS clinical trial (NCT04625907).[27] Most adoptive CAR cell trials in patients with solid tumors including RMS are still based on CAR T cells, with target antigens under evaluation including EGFR, HER2, and B7-H3 (CD276). One CAR T-cell trial targeting EGFR is specifically investigating non-central nervous system solid tumors in children and adolescents, including RMS (NCT03618381), but results are still pending.

EGFR as a potential antigen for CAR therapy is expressed by a larger proportion of RMS tumors than HER2 (ErbB2), another member of the EGFR family. HER2 has already been evaluated for targeted therapy of RMS with CAR-engineered T cells and cytokine-induced killer cells.[28 29] Although EGFR can be detected to some extent in FP-RMS,[11] it has mainly been identified as a marker for FN-RMS, particularly for a cellular subset with a progenitor signature. This subset is predominantly dormant and likely to resist treatment, potentially leading to disease recurrence and relapse.[30] These findings suggest a clinical relevance of EGFR as a therapeutic target for RMS.

Primary CAR NK cells targeting EGFR could be consistently generated and displayed potent cytotoxicity against EGFR-expressing RMS target cells of different sources (figures 1 and 2), which is in line with recent reports in glioblastoma and breast cancer.[31 32] Our data indicate that the high EGFR-CAR-specific efficacy was largely independent of the antigen dose, suggesting the attractive possibility of a low minimum antigen threshold (figure 2), and thus broad applicability of this approach in tumor therapy. Superior cytotoxic function of EGFR-CAR NK cells compared with NT NK cells was also validated at lower E:T ratios (figure 2B) and against 3D RMS spheroids (figure 2C). Importantly, experiments with chemotherapy-resistant RMS cell lines and patient-derived primary tumor cells from a patient with FP-RMS with progressive disease clearly confirmed potent and specific cytotoxicity of EGFR-CAR NK cells against RMS (figure 3).

The increased expression of individual activating NK cell ligands on chemotherapy-resistant RMS cells highlights the potential of combining chemotherapy with NK cell-based immunotherapy. This combination could synergistically improve antitumor responses by sensitizing RMS cells to NK cell immunotherapy.

While Patel *et al* reported that a subset of FN-RMS characterized by increased drug resistance is dependent on EGFR signaling and therefore susceptible to EGFR inhibition,[14] EGFR-CAR NK cells only depend on the presence of EGFR on the target cell surface regardless of its signaling and activation state. Thus, the CAR NK cell approach may be more widely applicable than EGFR blockade.

Nevertheless, despite its remarkable potency in vitro against RMS cells growing in 2D culture or as 3D spheroids, initial in vivo analyses did not yield similarly encouraging data. Following multiple injections of EGFR-CAR NK cells in an advanced-stage localized disease model, no significant effect on tumor growth was observed (online supplemental figure S3). In contrast, prolonged survival has been reported on repetitive administration of HER2-CAR NK-92 cells targeting FP-RMS in a systemic RMS xenograft model, mimicking early metastatic disease.[33] Similarly, treatment at very early stages of the disease, either on the same day or 1 day after tumor inoculation, resulted in some therapeutic benefit in systemic RMS models.[33 34] In contrast, tumors in advanced-stage RMS models seem no longer accessible to CAR NK cell monotherapy.

As it is well known that the TME in solid tumors presents a significant challenge for successful immunotherapy because it can hinder the effectiveness of cytotoxic immune cells and their migration to the tumor bed,[35] NK cell homing was examined. Thereby, we observed that EGFR-CAR NK cells rapidly migrated to the tumors, with a significantly higher proportion of EGFR-CAR NK cells persisting at the tumor site over a 5-day observation period compared with NT NK cells (figure 4). Nevertheless, no infiltration deep into the solid tumor mass was observed,

highlighting the need for combination strategies that enable efficient NK cell penetration and functionality.

Radiotherapy, a common treatment modality for various solid tumors, can not only damage cancer cells directly, but also modify the TME, with increasing evidence indicating enhanced immune cell infiltration after radiation treatment.[36 37] Several preclinical studies investigated the combined use of CAR T cells and radiotherapy for the treatment of solid tumors, with encouraging results.[38] Enhanced NK cell infiltration into tumors after radiotherapy has also been linked to improved clinical outcome in several malignancies, including colorectal cancer, pancreatic ductal adenocarcinoma, and cervical cancer.[39 40] These studies demonstrated that patients with higher levels of NK cell infiltration in their tumors following radiotherapy tended to experience better overall survival, suggesting that NK cells might facilitate or at least contribute to the therapeutic effects of radiotherapy. Radiotherapy significantly enhanced NK cell-mediated cytotoxicity against RMS in vitro, in both monolayer and 3D spheroid models, suggesting that radiotherapy sensitizes RMS cells to NK cell-mediated killing (figure 5A–D). These findings are consistent with prior studies indicating that radiotherapy can reprogram the TME to favor immune cell infiltration and activity.[41] Beyond direct cytotoxic effects, irradiation modulated the TME by altering chemokine profiles. Notably, IL-8 (CXCL8) levels were significantly increased following irradiation in both RMS monolayer and 3D spheroid cultures (figure 5E,F). IL-8 is a pro-inflammatory chemokine known to promote immune cell recruitment through CXCR1/CXCR2 signaling.[42] Of note, elevated IL-8 levels have been associated with enhanced NK cell infiltration, especially CD56$^{dim}$ cytotoxic NK cells, and improved antitumor responses in various cancer models.[41–43] However, IL-8 has also been shown to impair NK cell cytotoxicity in a STAT3-dependent manner in esophageal squamous cell carcinoma, suggesting context-dependent effects.[44] Furthermore, CCL2 was consistently upregulated in supernatants from NK cell-treated conditions (figure 5E,F). While CCL2 is a chemokine associated with monocyte recruitment, it also facilitates NK cell migration.[45 46] Its increased presence suggests a potential role for NK cells in shaping the inflammatory TME through chemokine release, potentially enhancing their own recruitment and activity. Nevertheless, sustained high CCL2 levels within the TME have been associated with NK cell dysfunction and impaired cytotoxic activity.[47] In vivo, radiotherapy promoted NK cell migration to RMS tumors (figure 5G–I), suggesting that radiation-induced chemokine expression may facilitate NK cell trafficking.

Further mechanistic studies are required to analyze the contributions of chemokines in modulating NK cell function and tumor infiltration in the context of RMS in vivo, especially in an immunocompetent setting.

We next examined whether enhanced NK cell infiltration following radiotherapy could translate into improved therapeutic outcomes in vivo. The combination of radiotherapy and adoptive NK cell therapy enabled NK cell penetration into the solid tumor mass, which was impaired if NK cell therapy was applied alone (figure 6H). Furthermore, in an s.c. RMS xenograft model, the combination of radiation and EGFR-CAR NK cells led to a transient reduction in absolute tumor size and overall delayed tumor outgrowth (figure 6B–F), thus providing a promising basis for further exploration of the therapeutic potential of this approach. These observations are in line with findings from canine sarcoma and triple-negative breast cancer xenograft models, where the combination of radiotherapy with adoptive NK cell transfer enhanced NK cell homing and cytotoxicity.[48 49] Furthermore, in a clinical trial with patients with pancreatic cancer investigating a combination of radiochemotherapy and the antibody-dependent cellular cytotoxicity-mediating antibody cetuximab, radiotherapy resulted in recruitment of NK cells to the tumor bed in a CXCL8-dependent manner.[43] In addition, Ames et al demonstrated that radiation increased the expression of NK cell-activating ligands, particularly in tumor cells exhibiting cancer stem cell-like properties, making them more susceptible to NK cell therapy.[50] Nevertheless, further investigation is needed to explore the detailed mechanism underlying the sensitizing effect of radiotherapy in the context of RMS.

CAR-engineered NK cells represent a potent alternative for CAR T-cell therapy due to their inherent natural cytotoxicity, favorable safety profile and potential as an allogeneic off-the-shelf product. Nevertheless, challenges persist regarding the optimal NK cell source and the development of scalable manufacturing processes suitable for clinical translation.[51] Cryopreservation remains a critical barrier to widespread clinical applicability, as it can impact viability, cytotoxic function, and phenotypic stability. Mark et al demonstrated that cryopreservation diminishes the motile fraction of peripheral blood (PB)-derived NK cells after thawing, thereby reducing their functionality compared with freshly prepared NK cells.[52] In contrast, Pfefferle et al revealed that PB-derived CAR-NK cells were less prone to cryo-induced apoptosis than umbilical cord blood-derived NK cells.[53] In this study, short-term cryopreserved NK cells retained comparable functionality and CAR expression to freshly prepared NK cells (online supplemental figure S7). However, a comparative analysis of their in vivo efficacy was not performed. To enhance post-thaw recovery, strategies such as cytokine priming are under investigation. Pretreatment with IL-15 and IL-18 has been shown to prevent cryopreservation-induced cell death by preventing granzyme B leakage from cytotoxic granules.[54] Additionally, ongoing efforts aim to optimize CAR constructs and integrate cytokine support to improve NK cell persistence and function in vivo. Taken together, our study demonstrated the successful generation of EGFR-targeting primary CAR NK cells that efficiently eliminated RMS cells growing in 2D culture or as 3D spheroids in vitro and inhibited the growth of RMS tumors in a xenograft in vivo model when combined with

fractionated radiation. This warrants further exploration of this approach as a treatment strategy for advanced RMS and possibly other malignancies with high medical need that are characterized by EGFR expression.

**Author affiliations**
[1]Department of Pediatrics, Experimental Immunology and Cell Therapy, Goethe University Frankfurt, Frankfurt (Main), Germany
[2]Frankfurt Cancer Institute, Goethe University Frankfurt, Frankfurt (Main), Germany
[3]University Cancer Center Frankfurt (UCT), University Hospital Frankfurt, Goethe University Frankfurt, Frankfurt (Main), Germany
[4]German Cancer Consortium (DKTK), partner site Frankfurt/Mainz, Frankfurt (Main), Germany
[5]Institute for Transfusion Medicine and Immunohematology, Goethe University Frankfurt, Frankfurt (Main), Germany
[6]University Hospital, Department of Radiotherapy and Oncology, Goethe University Frankfurt, Frankfurt (Main), Germany
[7]Institute for Experimental Pediatric Hematology and Oncology, Goethe University Frankfurt, Frankfurt (Main), Germany
[8]Dr Petra Joh-Haus, Frankfurter Stiftung für krebskranke Kinder, Frankfurt (Main), Germany
[9]School of Natural Sciences, University of Kent, Canterbury, UK
[10]German Red Cross Blood Donation Service Baden-Württemberg-Hessen, Institute Frankfurt, Frankfurt (Main), Germany
[11]Department of Pediatric and Perinatal Pathology, Dr Senckenberg Institute of Pathology, Goethe University Frankfurt, Frankfurt (Main), Germany
[12]Georg-Speyer-Haus, Institute for Tumor Biology and Experimental Therapy, Frankfurt (Main), Germany

**Competing interests** EU has a sponsored research project with Gilead and BMS and acts as a medical advisor for Phialogics and CRIION. HB has obtained research support from Bayer, Chugai, Erydel, Fresenius, Miltenyi, Sandoz-Hexal (a Novartis Company), Terumo BCT, honoraria or speakers' fees from BMS/Celgene, Fresenius, Kiadis, Miltenyi, Novartis, has served as consultant or on advisory boards of Apriligen, Arensia, Boehringer Ingelheim Vetmed, BMS/Celgene, Editas, medac, NMDP, Novartis, Sandoz-Hexal, receives royalties from medac and owns stock from Healthineers. The other authors have no competing interests to declare.

**Patient consent for publication** Not applicable.

**Ethics approval** This study involves human participants and was approved by the Ethics Committee of Goethe University, Frankfurt am Main, Germany. Approval numbers: SPO-04-2015, 329/10, and 274/18. Participants gave informed consent to participate in the study before taking part.

**Provenance and peer review** Not commissioned; externally peer reviewed.

**Data availability statement** All data relevant to the study are included in the article or uploaded as supplementary information.

**ORCID iDs**
Lisa Marie Reindl http://orcid.org/0000-0002-1027-1256
Tobias Bexte http://orcid.org/0009-0009-2392-6416
Stephanie Hehlgans http://orcid.org/0000-0002-6816-3450
Halvard Bonig http://orcid.org/0000-0003-0088-2675
Meike Vogler http://orcid.org/0000-0003-2650-586X
Franz Rödel http://orcid.org/0000-0001-6057-1022
Winfried S Wels http://orcid.org/0000-0001-9858-3643
Evelyn Ullrich http://orcid.org/0000-0001-8530-1192

**REFERENCES**
1 Hawkins DS, Spunt SL, Skapek SX, et al. Children's Oncology Group's 2013 blueprint for research: Soft tissue sarcomas. *Pediatr Blood Cancer* 2013;60:1001–8.
2 Evans C, Shepherd L, Bryan G, et al. A systematic review of early phase studies for children and young people with relapsed and refractory rhabdomyosarcoma: The REFoRMS-SR project. *Int J Cancer* 2024;154:1235–60.
3 Heske CM, Mascarenhas L. Relapsed Rhabdomyosarcoma. *J Clin Med* 2021;10:804.
4 Vivier E, Rebuffet L, Narni-Mancinelli E, et al. Natural killer cell therapies. *Nature New Biol* 2024;626:727–36.
5 Reindl LM, Albinger N, Bexte T, et al. Immunotherapy with NK cells: recent developments in gene modification open up new avenues. *Oncoimmunology* 2020;9:1777651.
6 Wendel P, Reindl LM, Bexte T, et al. Arming Immune Cells for Battle: A Brief Journey through the Advancements of T and NK Cell Immunotherapy. *Cancers (Basel)* 2021;13:1481.
7 Marin D, Li Y, Basar R, et al. Safety, efficacy and determinants of response of allogeneic CD19-specific CAR-NK cells in CD19+ B cell tumors: a phase 1/2 trial. *Nat Med* 2024;30:772–84.
8 Liu E, Marin D, Banerjee P, et al. Use of CAR-Transduced Natural Killer Cells in CD19-Positive Lymphoid Tumors. *N Engl J Med* 2020;382:545–53.
9 Li T, Niu M, Zhang W, et al. CAR-NK cells for cancer immunotherapy: recent advances and future directions. *Front Immunol* 2024;15.
10 Wang W, Liu Y, He Z, et al. Breakthrough of solid tumor treatment: CAR-NK immunotherapy. *Cell Death Discov* 2024;10:40.
11 Ganti R, Skapek SX, Zhang J, et al. Expression and genomic status of EGFR and ErbB-2 in alveolar and embryonal rhabdomyosarcoma. *Mod Pathol* 2006;19:1213–20.
12 Lynch TJ, Bell DW, Sordella R, et al. Activating mutations in the epidermal growth factor receptor underlying responsiveness of non-small-cell lung cancer to gefitinib. *N Engl J Med* 2004;350:2129–39.
13 Yarden Y, Sliwkowski MX. Untangling the ErbB signalling network. *Nat Rev Mol Cell Biol* 2001;2:127–37.
14 Patel AG, Chen X, Huang X, et al. The myogenesis program drives clonal selection and drug resistance in rhabdomyosarcoma. *Dev Cell* 2022;57:1226–40.
15 Ricci C, Polito L, Nanni P, et al. HER/erbB receptors as therapeutic targets of immunotoxins in human rhabdomyosarcoma cells. *J Immunother* 2002;25:314–23.
16 Müller S, Bexte T, Gebel V, et al. High Cytotoxic Efficiency of Lentivirally and Alpharetrovirally Engineered CD19-Specific Chimeric Antigen Receptor Natural Killer Cells Against Acute Lymphoblastic Leukemia. *Front Immunol* 2019;10:3123.

17 Albinger N, Pfeifer R, Nitsche M, *et al*. Primary CD33-targeting CAR-NK cells for the treatment of acute myeloid leukemia. *Blood Cancer J* 2022;12:61.

18 Genßler S, Burger MC, Zhang C, *et al*. Dual targeting of glioblastoma with chimeric antigen receptor-engineered natural killer cells overcomes heterogeneity of target antigen expression and enhances antitumor activity and survival. *Oncoimmunology* 2016;5:e1119354.

19 Wels W, Beerli R, Hellmann P, *et al*. EGF receptor and p185erbB-2-specific single-chain antibody toxins differ in their cell-killing activity on tumor cells expressing both receptor proteins. *Int J Cancer* 1995;60:137–44.

20 Wagner J, Pfannenstiel V, Waldmann A, *et al*. A Two-Phase Expansion Protocol Combining Interleukin (IL)-15 and IL-21 Improves Natural Killer Cell Proliferation and Cytotoxicity against Rhabdomyosarcoma. *Front Immunol* 2017;8:676.

21 Rudzinski ER, Anderson JR, Lyden ER, *et al*. Myogenin, AP2β, NOS-1, and HMGA2 are surrogate markers of fusion status in rhabdomyosarcoma: a report from the soft tissue sarcoma committee of the children's oncology group. *Am J Surg Pathol* 2014;38:654–9.

22 Borinstein SC, Steppan D, Hayashi M, *et al*. Consensus and controversies regarding the treatment of rhabdomyosarcoma. *Pediatr Blood Cancer* 2018;65:e26809.

23 Chen C, Dorado Garcia H, Scheer M, *et al*. Current and Future Treatment Strategies for Rhabdomyosarcoma. *Front Oncol* 2019;9:1458.

24 Oberlin O, Rey A, Sanchez de Toledo J, *et al*. Randomized comparison of intensified six-drug versus standard three-drug chemotherapy for high-risk nonmetastatic rhabdomyosarcoma and other chemotherapy-sensitive childhood soft tissue sarcomas: long-term results from the International Society of Pediatric Oncology MMT95 study. *J Clin Oncol* 2012;30:2457–65.

25 Rosenberg AR, Anderson JR, Lyden E, *et al*. Early response as assessed by anatomic imaging does not predict failure-free survival among patients with Group III rhabdomyosarcoma: A report from the Children's Oncology Group. *Eur J Cancer* 2014;50:816–23.

26 Morel VJ, Rössler J, Bernasconi M. Targeted immunotherapy and nanomedicine for rhabdomyosarcoma: The way of the future. *Med Res Rev* 2024;44:2730–73.

27 Chisholm J, Mandeville H, Adams M, *et al*. Frontline and Relapsed Rhabdomyosarcoma (FaR-RMS) Clinical Trial: A Report from the European Paediatric Soft Tissue Sarcoma Study Group (EpSSG). *Cancers (Basel)* 2024;16:998.

28 Merker M, Pfirrmann V, Oelsner S, *et al*. Generation and characterization of ErbB2-CAR-engineered cytokine-induced killer cells for the treatment of high-risk soft tissue sarcoma in children. *Oncotarget* 2017;8:66137–53.

29 Hegde M, Joseph SK, Pashankar F, *et al*. Tumor response and endogenous immune reactivity after administration of HER2 CAR T cells in a child with metastatic rhabdomyosarcoma. *Nat Commun* 2020;11:3549.

30 Danielli SG, Wei Y, Dyer MA, *et al*. Single cell transcriptomic profiling identifies tumor-acquired and therapy-resistant cell states in pediatric rhabdomyosarcoma. *Nat Commun* 2024;15:6307.

31 Ma R, Lu T, Li Z, *et al*. An Oncolytic Virus Expressing IL15/IL15Rα Combined with Off-the-Shelf EGFR-CAR NK Cells Targets Glioblastoma. *Cancer Res* 2021;81:3635–48.

32 Liu Y, Zhou Y, Huang K-H, *et al*. Targeting epidermal growth factor-overexpressing triple-negative breast cancer by natural killer cells expressing a specific chimeric antigen receptor. *Cell Prolif* 2020;53:e12858.

33 Heim LM, Moser LM, Kreyenberg H, *et al*. ErbB2 (HER2)-CAR-NK-92 cells for enhanced immunotherapy of metastatic fusion-driven alveolar rhabdomyosarcoma. *Front Immunol* 2023;14:1228894.

34 Vela M, Bueno D, González-Navarro P, *et al*. Anti-CXCR4 Antibody Combined With Activated and Expanded Natural Killer Cells for Sarcoma Immunotherapy. *Front Immunol* 2019;10:1814.

35 Stojanovic A, Correia MP, Cerwenka A. Shaping of NK cell responses by the tumor microenvironment. *Cancer Microenviron* 2013;6:135–46.

36 Weichselbaum RR, Liang H, Deng L, *et al*. Radiotherapy and immunotherapy: a beneficial liaison? *Nat Rev Clin Oncol* 2017;14:365–79.

37 Zhang Z, Liu X, Chen D, *et al*. Radiotherapy combined with immunotherapy: the dawn of cancer treatment. *Sig Transduct Target Ther* 2022;7:258.

38 He J, Yan Y, Zhang J, *et al*. Synergistic treatment strategy: combining CAR-NK cell therapy and radiotherapy to combat solid tumors. *Front Immunol* 2023;14:1298683.

39 Parikh AR, Szabolcs A, Allen JN, *et al*. Radiation therapy enhances immunotherapy response in microsatellite stable colorectal and pancreatic adenocarcinoma in a phase II trial. *Nat Cancer* 2021;2:1124–35.

40 Liu C, Li X, Huang Q, *et al*. Single-cell RNA-sequencing reveals radiochemotherapy-induced innate immune activation and MHC-II upregulation in cervical cancer. *Signal Transduct Target Ther* 2023;8:44.

41 Lin X, Liu Z, Dong X, *et al*. Radiotherapy enhances the anti-tumor effect of CAR-NK cells for hepatocellular carcinoma. *J Transl Med* 2024;22:929.

42 Campbell JJ, Qin S, Unutmaz D, *et al*. Unique Subpopulations of CD56+ NK and NK-T Peripheral Blood Lymphocytes Identified by Chemokine Receptor Expression Repertoire. *J Immunol* 2001;166:6477–82.

43 Walle T, Kraske JA, Liao B, *et al*. Radiotherapy orchestrates natural killer cell dependent antitumor immune responses through CXCL8. *Sci Adv* 2022;8:eabh4050.

44 Wu J, Gao F-X, Wang C, *et al*. IL-6 and IL-8 secreted by tumour cells impair the function of NK cells via the STAT3 pathway in oesophageal squamous cell carcinoma. *J Exp Clin Cancer Res* 2019;38:321.

45 O'Sullivan T, Saddawi-Konefka R, Gross E, *et al*. Interleukin-17D mediates tumor rejection through recruitment of natural killer cells. *Cell Rep* 2014;7:989–98.

46 van Helden MJG, Zaiss DMW, Sijts AJAM. CCR2 defines a distinct population of NK cells and mediates their migration during influenza virus infection in mice. *PLoS One* 2012;7:e52027.

47 Xu X, Wang Q, Deng B, *et al*. Monocyte Chemoattractant Protein-1 Secreted by Decidual Stromal Cells Inhibits NK Cells Cytotoxicity by Up-Regulating Expression of SOCS3. *PLoS ONE* 2012;7:e41869.

48 Canter RJ, Grossenbacher SK, Foltz JA, *et al*. Radiotherapy enhances natural killer cell cytotoxicity and localization in pre-clinical canine sarcomas and first-in-dog clinical trial. *J Immunother Cancer* 2017;5:98.

49 Kim KW, Jeong J-UK, Lee K-H, *et al*. Combined NK Cell Therapy and Radiation Therapy Exhibit Long-Term Therapeutic and Antimetastatic Effects in a Human Triple Negative Breast Cancer Model. *Int J Radiat Oncol Biol Phys* 2020;108:115–25.

50 Ames E, Canter RJ, Grossenbacher SK, *et al*. Enhanced targeting of stem-like solid tumor cells with radiation and natural killer cells. *Oncoimmunology* 2015;4:e1036212.

51 Daher M, Melo Garcia L, Li Y, *et al*. CAR-NK cells: the next wave of cellular therapy for cancer. *Clin & Trans Imm* 2021;10:e1274.

52 Mark C, Czerwinski T, Roessner S, *et al*. Cryopreservation impairs 3-D migration and cytotoxicity of natural killer cells. *Nat Commun* 2020;11:5224.

53 Pfefferle A, Contet J, Wong K, *et al*. Optimisation of a primary human CAR-NK cell manufacturing pipeline. *Clin & Trans Imm* 2024;13:e1507.

54 Berjis A, Muthumani D, Aguilar OA, *et al*. Pretreatment with IL-15 and IL-18 rescues natural killer cells from granzyme B-mediated apoptosis after cryopreservation. *Nat Commun* 2024;15:3937.